International Journal of Sustainable and Green Energy
2024, Vol. 13, No. 4, pp. 67-81
https://doi.org/10.11648/j.ijrse.20241304.11

Research Article

Parameters Estimation and Curves Analysis for Faults Evaluation of a Degraded Photovoltaic Module

Albert Ayang[1], Deli Goron[1], Fabrice Kwefeu Mbakop[1], Yaouba[1, 2, *]

[1]Department of Renewable Energy, National Advance School of Engineering of Maroua, University of Maroua, Maroua, Cameroon

[2]Research Centre for Renewable Energy, Institute of Geological and Mining Research, Yaoundé, Cameroon

Abstract

In the present work, a fault evaluation method for photovoltaic arrays based on fault parameters identification and curves analysis is proposed for diagnosing the state of photovoltaic generators. An overview of the components, the modelling of the photovoltaic generator and the meaning of the parameters is established for relating parameters to photovoltaic components and environmental conditions. The analysis and investigation of the relationship between the maximum power points and the parameters variations are performed. Investigation on how degradations and failure on photovoltaic systems can affect parameters, is established. In this context, the methodology for diagnosing and monitoring defects based on photovoltaic estimated parameters is developed; the optimization technique maximum likelihood, is used for extracting health and faults parameters from the measured curves of the photovoltaic array. From residual vectors, the parameters which vary more are the series resistance, the shunt resistor, and the current of photon. The maximum power also changes and decreases from its reference value. The validation results prove deviations on parameters, which means that there are degradations and failures on the ARCO Solar M75 array after 20 years of outdoors operation. So, at the end of this analysis, it is recommended to act on the PV system through junction box, cell edges, wiring, busbars, and connectors.

Keywords

Parameter Estimation, Curves Analysis, PV Module, Degradations, Failure, Maximum Likelihood Estimator (MLE), Fault Diagnosis

1. Introduction

Understanding photovoltaic (PV) generator degradations and failure for design, monitoring and supervision of PV systems still very important. The analysis of degradation and failure mechanisms of PV generators is an important key to ensure lifetimes exceeding 25 years. However photovoltaic (PV) generators are known for their reliability, some modules degrade or even fail when operating outdoors for short or extended periods. Electricity generated using PV technology can only be profitable if the PV generators operate reliably for 25–30 years under field conditions [1]. The long-term reliability of PV modules is crucial for their commercial success, as it is one of the key factors affecting the cost of PV electricity.

Over the past decade, the PV market has experienced

*Corresponding author: yaoubadams21@gmail.com (Yaouba)

Received: 1 October 2024; **Accepted:** 28 October 2024; **Published:** 18 November 2024

unprecedented growth. For an energy need, a PV system can only be effective if an installation is optimized and maintained. Currently, failures leading to a degradation of a module are not considered because of the difficulty of measuring the power of a single module in a PV system, and the lack of information on the various degradations and failure modes of PV modules. Investors require the most precise estimates of PV modules lifetime to develop accurate model's investment costs and returns. Monitoring PV system degradation is important because a high degradation rate and serious failures lead directly to a loss of power output and therefore a reduction in the return on investment, and an increase in the financial risk [2, 3]. PV plant operators must be aware of the degradation mechanisms to design appropriate maintenance plans, and, when necessary, claim to the manufacturers.

PV systems should be monitored to control their production and detect any possible faults. Diagnosis methods can be categorized into two groups: nonelectric methods such as visual (fading, owning, surface soiling, delamination, etc.) and thermal (extraordinary heating, etc.), and electric methods (dark/illuminated current voltage measurement, transmittance line diagnosis, radio frequency RF measurement, etc.). Among these methods, the non-electric methods need frequent visual checks of the PV array to observe the color changes of the modules or the thermal properties such as hot spots. These methods need a system of thermal cameras in front of the PV array. On the contrary, the electrical methods need only the measurement of the electrical output signature such as voltage and current or power [4]. Thus, fault diagnosis using electrical methods is more advantageous and promising for the monitoring and diagnostic of PV systems [5].

Over the past decade, different aspects of fault detection techniques for PV systems were reported. Most of them use local sensors to measure temperature and irradiance; some instead use satellite data [7], which, however, seems to be less accurate. Another common point of most of the monitoring systems is that they analyze data from the PV generator, limiting the range of possible faults that can be detected. Moreover, most of them analyze only the energy production [8]. These systems can defect general failures, such as constant energy losses, total blackout, short-term energy losses [8] and, in the best cases, are able to detect shadowing [6]. However, such systems are not able to detect the cause of the fault.

The introduction of the concept of distributed maximum power point tracking (power optimizers are used on the single panel level), has achieved a new level of control and supervision of PV systems by parameters extraction, in which the point of the fault and the causes of power losses can be determined [8, 9]. The monitoring of the key PV module parameters would reflect the changes in the PV generator's health state. Changes due to degradations and failures of the parameters can seriously affect the PV system stability and the operation of various control devices. These parameters variations should be extracted from the (I-V) and/or (P-V) curves variations. Estimating the model parameters of the PV generator could lead to accomplish a diagnostic tool and to estimate several factors that affect the health state of a PV generator. In this context, it is crucial to look for an extraction technique that performs this evaluation precisely and quickly. Several techniques have been developed for the residue generation, among them the parametric techniques that lead to parameter estimation. This leads to the introduction of modelling and fault diagnosis of PV systems based on the estimation of PV module parameters.

The maximum likelihood estimator (MLE) algorithm, as new estimation approach, is proposed for extracting the unknown parameters of a PV generator [10, 11]. The contributions of the present paper are to: (i) extend the application of this method for faults detection and diagnosis of PV generators (ii) verify experimentally the accuracy of the proposed estimator MLE algorithm at nominal operating condition tests (NOCT) of PV generators (iii) establish a diagnosis and monitoring methodology of the PV generator using information from extracted parameters.

The key role of this method is to detect parameters deviations and to evaluate the health state of the PV generator. The estimation should assess all parameters of PV modules to analyze any observed degradation or failure. These parameters variations should be estimated from (I, V, P) data collected by sensors. The failure pattern would be presumed from the parameter's variations caused by (I-V) curve variations if the field data were accumulated. The calculated parameters are used not only to detect age-related failures or degradations, but also to build (I-V) or (P-V) curves references when mismatched modules and serious failures occurred. In this paper data are obtained from the ARCO Solar M75 array at nominal operating condition tests (NOCT) which is evaluated in 1990, reevaluated in 2001 and 2010. The module was installed in 1990 by the Schatz Energy Research Center. For the past 20 years the array has continued to operate in a cool environment and the performance of each module was reevaluated in 2001 and again in 2010 [12-14].

The rest of the paper is organized as follows: Section 2 briefly presents an overview of the PV generator components, the electrical model and the characteristics of the PV generator, and the meaning of the parameters. Section 3 outline analysis and investigation of the relationship between the maximum power points and parameters. Section 4 presents an investigation of degradation, failure modes and effects on parameters. Section 5 presents the procedure of fault diagnosis and monitoring method based on parameters and (I-V) and (P-V) curves analysis. Section 6 discusses parameters identification, residual generators, fault diagnosis and monitoring results from the ARCO Solar M75 array at NOCT in 1990, 2001 and 2010. Finally, Section 7 provides conclusion to this work.

2. PV Generators: Components, Modeling and Meaning of Parameters

The photovoltaic module consists of PV cells, an encapsulate, bypass diodes, connectors, a junction box, a cable, a protective glass on the front face of the module and a glass or a polymer film (Tedlar generally) on the rear side of the module (Figure 1). The assembly of these components can protect the cells against different contacts and against environmental conditions such as humidity and high temperature, which can cause degradations and failures.

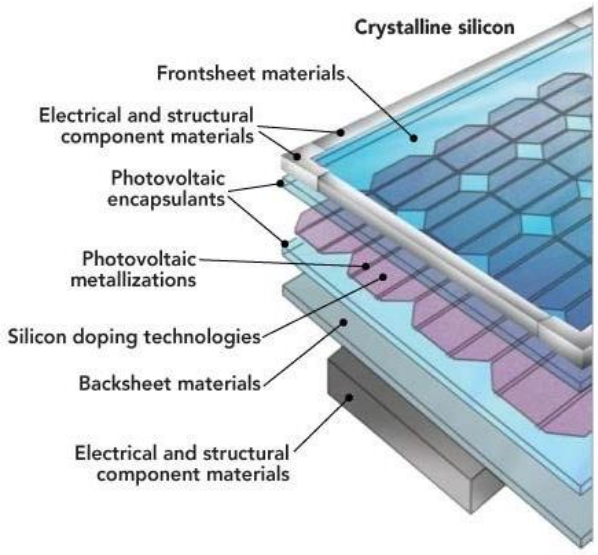

Figure 1. *Sectional view of a PV module [15].*

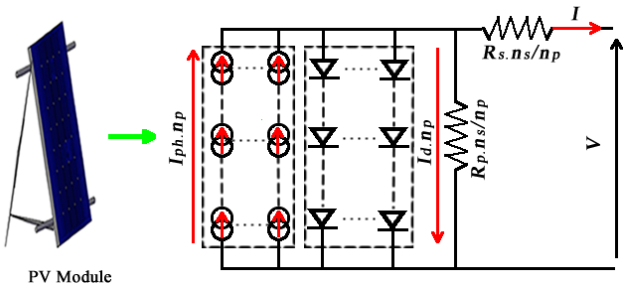

Figure 2. *Module composed of n series and p parallel cells.*

Several models have been introduced and have made it possible to represent the behavior of the solar generator systems by considering many physical variables. Among them, the single-diode model is much more common to use [16], as described by (1) and its equivalent electrical circuit model shown in Figure 2.

$$I = I_{ph} - I_o\left[\exp\left((V+R_sI)/nV_T\right)-1\right]-\left(V+R_sI\right)/R_p \quad (1)$$

As described in [10, 11], five unknown parameters are to be identified, namely the photo current (I_{ph}), the saturation current (I_o); the series resistance (R_s); the shunt resistance (R_p), and the diode ideality factor (n). It is necessary to know how these parameters are part of the external and the internal components of the PV generator.

The series resistance R_s of the PV generator represents the sum of the resistances contributed by all of the series-connected cell layers, the interconnect bus-bars contacts, the resistances in junction-box terminations and the wiring between both ends of the system's circuit [17]. The series resistance reduces the voltage produced by the cell, which ultimately reduces the performance of the PV cell, and hence the module/array. The value of series resistance is affected by the changes in resistance of any of these components and subcomponents of the PV system. Increases in series resistance are linked to corrosion inside modules and connectors, UV degradation of silicon, and other material degradation processes that contribute to the overall degradation of PV system performance [18].

The shunt resistance, R_p , is caused by any parallel high-conductivity paths (shunts) through the solar cell or on the cell edges [19]. These would be due to crystal damage and impurities in and near the junctions and would give rise to the shunt current.

Ideality factor n expresses the degree of ideality of the diodes incorporated in the PV generator. Usually, $1 \le n \le 2$ and the choice depends on other parameters of the (I-V) model.

The saturation current I_0 expresses the saturation current of the diode of the PV generator. It depends mainly on temperature [20].

The photo current I_{ph} expresses the current generated directly by irradiation on the PV generator. The photo current $I_{ph,ref}$ at the STC is related to the short circuit current $I_{sc,ref}$ at the STC, by the following expression [21].

$$I_{ph,ref} \approx I_{sc,ref}\left(1+R_s/R_P\right) \quad (2)$$

For an ideal generator $R_s \approx 0$, $R_P \approx +\infty$, equation 2 becomes:

$$I_{sc,ref} \approx I_{ph,ref} \quad (3)$$

$$I_{ph} \approx \alpha I_{sc}, \ \alpha \ge 1 \quad (4)$$

Assuming that $I_{sc,ref}$ is generally given by the manufacturer and considering (3), if R_p decreases (due to crystal damage and impurities in and near the junction…), and if R_s increases (bad contact resulting from corrosion…), then I_{ph}

increases as illustrated by (4).

3. Overview of Degradation, Failure, and Effects on Parameters

Degradation is the gradual deterioration of the characteristics of a component or a system which may affect its ability to operate within the limits of acceptability criteria and which is caused by the operating conditions [23]. The energy produced by a PV system depends on various factors such as nominal characteristics of the system components, electrical and geometrical configurations, and weather conditions of the installation site, shadowing, PV plant availability, degradations and faults that may occur during normal operations [24]. The performance of a PV generator can be degraded due to several factors such as temperature, humidity, irradiation, mechanical shock [25], etc. Each one of these various named factors may induce one or more types of module degradation and failures. Many authors have investigated the usual causes of degradation, and failure of a PV generator after prolonged exposure in the field. Tables 1 and 2, respectively, summarize the most frequent PV generator degradation modes under material aging and failure modes found in the literature [26]. A degraded PV generator may keep doing its primary function, which is to generate electricity from sunlight, even if its use is no longer optimal. Degradation and failure phenomena vary significantly between cells, modules and installations, resulting in different reported power degradation rates. The main defects observed in the field-aged PV modules include EVA browning, degradation of the antireflective coating, delamination between the glass encapsulates and the cell-encapsulated interfaces, humidity ingress, corrosion of busbars and contacts, shunt paths, cracks/micro-cracks in the cell, damage of the glass and the back sealing, and bypass diode failure. However, the degraded state of the module can be more problematic when the degradation exceeds a critical threshold [27].

Investigations show that degradation modes due to aging are responsible for lower performance and changes of parameters. These degradation modes are [26, 28-35]:

1) Front surface soiling;
2) Optical degradation or discolouration of the encapsulating material;
3) Degradation of anti reflection (AR) coating;
4) Light induced degradation;
5) Corrosion and temperature induced degradation.

If there is no protection, the PV generator degradations could cause serious failures or breakdown as listed in Table 2. This summary table carries out failures and causes, effects on maximum power, and parameters. Diagnosis and detection modes related to these failures, found in the literature, are also listed.

Identifying the physical location of the failure is the first step in the analysis of the critical failure modes, which are listed below [33-35]:

1) Mismatched PV generators;
2) Cells degradation;
3) Module delamination;
4) Module glass breakages and Cracking Cells;
5) Hot spot failure;
6) Interconnect open-circuit PV generators;
7) Short-circuited PV generators or line-line fault;
8) Bypass diode failure;
9) Ground faults.

In this paper, the evaluation of the residual generator of the parameters for the monitoring and supervision of a PV generator during operation is proposed. This diagnosis method prevents some cases of degradations and failures as mentioned in tables 1 and 2.

Table 1. *Degradations caused by material aging after prolonged exposure in field conditions.*

Degradations	Front surface soiling	Optical degradation or discoloration of the encapsulating material	Degradation of anti-reflection (AR) coating	Light induced degradation	Corrosion and temperature induced degradation
Causes	Dirt accumulation on the module's	-UV exposure - Elevated temperature and humidity -Diffusion of dirt and moisture ingress -Browning, yellowing and whiting of EVA layer	- Inter diffusion of species from cell's emitter region to the AR coating and vice versa - Manufacturer defects	Broken bonds by energy release during recombination of electron hole pairs	Elevated modules temperature decrease
Types of failures if there is no protection.	-Partial shade - Hot spot damage - Mismatched cell/module/array	- Partial shade - Hot spot damage - Mismatched cell/module/array - Module delamination	- Cells degradation - Mismatched cell/module/array	-Meta stable defects -Material deterioration - Module delamination -Cell degradation	- Thermal stress -Material deterioration - Module delamination -Cell degradation

Degradations	Front surface soiling	Optical degradation or discoloration of the encapsulating material	Degradation of anti-reflection (AR) coating	Light induced degradation	Corrosion and temperature induced degradation
Effects on Pmax and on parameters	-Pmax and FF drops -Isc and Iph decrease -Unknown effects on Io,Rs,Rp,n	-Pmax and FF drops -Isc and Iph decrease -Unknown effects on Io,Rs,Rp,n	-Pmax and FF drops -Isc and Iph decrease -Voc decrease -Unknown effects on Io,Rs,Rp,n	-Pmax and FF drops -Isc and Iph decrease -Voc decrease -Rp decrease -Rs increase -Unknown effects on Io,n	-Pmax and FF drops -Isc and Iph slightly increase -Voc decrease -Rp decrease -Rs increase - n decrease - Io decrease
Protection actions	-Regular cleaning - Use of bypass diodes	-Use of stabilizer and anti-oxidants -Use of bypass diodes	- Texturing the surface - Adding AR coating -Use of bypass diodes	Use of bypass diodes	Use of bypass diodes
Adapted diagnosis, detection methods	-Visual inspection -Evaluation of residual generator and monitoring Isc,Io,Rs,Rp,n,Voc - (I-V) curves data measurements and analysis -Preventive and predictive maintenances	-Visual inspection -Evaluation of residual generator and monitoring Isc,Io,Rs,Rp,n,Voc - (I-V) curves data measurements and analysis -Preventive and predictive maintenances	- Visual inspection - Evaluation of residual generator and monitoring Isc,Io,Rs,Rp,n,Voc - (I-V) curves data measurements and analysis -Preventive and predictive maintenances	- Visual inspection -Evaluation of residual generator and monitoring Isc,Io,Rs,Rp,n,Voc - (I-V) curves data measurements and analysis -Preventive and predictive maintenances	- Visual inspection - Evaluation of residual generator and monitoring Isc,Io,Rs,Rp,n,Voc - (I-V) curves data measurements and analysis -Preventive and predictive maintenances

Table 1. *Summary of failures caused by accidents degradations modes or manufacturer defects on PV generator after years of outdoors operation.*

Failures	Cells degradations	Short circuit cell/modules	Interconnect open circuit cells/modules	Module glass breakage and cracking cell	Bypass diode failure	Hot spot failure	Module delamination	Ground faults	Mismatched cell/modules
Causes	-Light induced degradation -Temperature induced degradation -AR coating degradation	-Manufacturers' defects - Discolouration of the encapsulating material	-Damage during installation -Temperature degradation by thermal stress -Manufacturer's defects -Wind load	-Damage during installation -Temperature degradation by thermal stress -Manufacturers defects. -Wind load	-Overheating -Manufacturers defects	-Mismatched cell by front surface soiling Temperature degradation by thermal stress -Partial shade -manufacturers defects	-Hight temperature in mismatched cell -Front soiling surface -Moisture and thermal expansion -Shaded cell -manufacturers defects	-isolation of cabling isolation of junction box Connection within PV array-leakage currents	-Front surface soiling -Encapsuling degradation -Hot spot -AR coating deterioration -Partial shading manufacturers defects
Effects on Pmax and on parameters	-Pmax and FF drops -Isc and Iph slightly increase -Voc de-	-Pmax and FF drops -Isc and Iph slightly increase -Voc de-	-Pmax and FF drops -Isc and Iph decrease -Rs increase	-Pmax and FF drops -Isc and Iph decrease -Unknown effects on	-Pmax and FF drops -Isc and Iph decrease -Unknown effects on	-Pmax and FF drops -Isc and Iph decrease -Unknown effects on	-Pmax and FF drops -Unknown effects on Isc,Io,Rs,Rp, n	-Pmax and FF drops -Isc and Iph decrease -Rs increase	-Pmax and FF drops -Isc and Iph decrease -Voc de-

Failures	Cells degradations	Short circuit cell/modules	Interconnect open circuit cells/modules	Module glass breakage and cracking cell	Bypass diode failure	Hot spot failure	Module delamination	Ground faults	Mismatched cell/modules
	crease -Rp decrease -Rs increase - n decrease - Io decrease	crease -Rp decrease -Rs increase - n decrease - Io decrease	-Unknown effects on Io,Rp, n	Io,Rs,Rp, n	Io,Rs,Rp, n	Io,Rs,Rp, n		-Unknown effects on Io,Rp, n	crease -Unknown effects on Io,Rs,Rp,n
Adapted diagnosis, detection methods	-Visual inspection -thermal camera - (I-V) curves data measurements and analysis -Evaluation of residual generator and monitoring Isc,Io,Rs,Rp, n,Voc	-Visual inspection - (I-V) curves data measurements and analysis -Evaluation of residual generator and monitoring Isc,Io,Rs,Rp,n, Voc	-Visual inspection -thermal camera - (I-V) curves data measurements and analysis -Evaluation of residual generator and monitoring Isc,Io,Rs,Rp, n,Voc	-Visual inspection -thermal camera - (I-V) curves data measurements and analysis -Evaluation of residual generator and monitoring Isc,Io,Rs,Rp,n, Voc	-Visual inspection - (I-V) curves data measurements and analysis -Evaluation of residual generator and monitoring Isc,Io,Rs,Rp,n,Voc	-Visual inspection -thermal camera -hot spot endurance testing-individual cell temperature monitoring - (I-V) curves data measurements and analysis -Evaluation of residual generator and monitoring Isc,Io,Rs,Rp, n,Voc	-Visual inspection - (I-V) curves data measurements and analysis -Evaluation of residual generator and monitoring Isc,Io,Rs,Rp,n, Voc	-Visual inspection - (I-V) curves data measurements and analysis -Evaluation of residual generator and monitoring Isc,Io,Rs,Rp,n,Voc	-Visual inspection -thermal camera -hot spot endurance testing-individual cell temperature monitoring - (I-V) curves data measurements and analysis -Evaluation of residual generator and monitoring Isc,Io,Rs,Rp ,n,Voc

4. Fault Diagnosis and Monitoring Procedure Based on Estimated Parameters and Curves Analysis

When fault or degradation occurs, the changes in parameter values can be introduced in the modified electrical model, as described in the following equation:

$$I = \tilde{I}_{ph} - \tilde{I}_o\left[\exp\left((V + \tilde{R}_s I)/\tilde{n}V_T\right) - 1\right] - \left(V + \tilde{R}_s I\right)/\tilde{R}_p \quad (5)$$

where $\tilde{I}_{ph} = I_{ph} + \Delta I_{ph}$; $\tilde{I}_o = I_o + \Delta I_o$; $\tilde{R}_s = R_s + \Delta R_s$; $\tilde{n} = n + \Delta n$; $\tilde{R}_p = R_p + \Delta R_p$.

ΔI_{ph} , ΔI_o , Δn , ΔR_s , ΔR_p denote changes or deviations of the parameters (I_{ph} , I_0 , R_s , n , R_p). The vector $\Delta x = \left[\Delta I_{ph} \quad \Delta I_o \quad \Delta n \quad \Delta R_s \quad \Delta R_p\right]^T$ is defined as the residual vector of the parameters' variations.

The unknown parameters of a system are obtained with the maximum likelihood estimator (MLE) optimization technique.

4.1. Maximum Likelihood Estimator Method

The prediction approach based on the MLE, as a mathematical optimization technique, is chosen for the identification process. The MLE of the parameters' vector is the value of unknown parameters $x^* = x_{opt}$ that maximizes the joint

probability, $I(k,x)$, that is equal to the actual measurements $I_{meas}(k)$. It is also equivalent to the vector that minimizes the cost function (16) adapted for parameters estimation with process and measurement noise.

$$V(x)=\frac{1}{2}\sum_{k=1}^{N}\left(\varepsilon^{T}{}_{k}R(x)^{-1}\varepsilon_{k}\right)+\frac{1}{2}N\log\left(\det R(x)\right) \quad (6)$$

The optimum parameters $x^{*}=x_{opt}$ are those that satisfy following equation:

$$\nabla V=\left[\frac{\partial V}{\partial x}\right]_{x\to x^{*}}\approx 0 \quad (7)$$

∇V represents the cost function gradient, where $\varepsilon_k=I(k,x)-I_{meas}(k)$ and $R(x)=E\left(\varepsilon_k^{T}.\varepsilon_k\right)$. ε_k is the innovation sequence. It is also the residue or error in the current prediction at known voltages. $R_k(x)$ is the corresponding measurement noise covariance matrix. N denote the number of experimental measures.

The optimization problem could then be formulated as following:

$$\begin{cases}\min\ V(x)\\ subject\ to\begin{cases}x_{\min}\le x\le x_{\max}\\ x\ge 0\end{cases}\end{cases} \quad (8)$$

$$x=\left[I_{ph},I_o,R_s,n,R_p\right] \quad (9)$$

$x_{\max}$ and $x_{\min}$ are the upper and the lower bounds of the parameter vector x, respectively.

The trust region algorithm is used to find out the unknown parameters of the PV generator. A vector, described by (9), defines each solution.

Details on implementing the identification of the parameters using the MLE method are shown as a flowchart algorithm in Figure 3. The steps shown in Figure 4 describe the methodology adopted for detecting deviations of the parameters, hence detection of a fault or degradation of a PV module.

4.2. Details of Identification Steps

Details on implementing identification parameters using the MLE are shown in Figure 3. The first step is to model the PV module; this model is considered in a precise operating condition and initially set by initial values of the parameters as mentioned in the second step. Thirdly, the model is solved by Newton Raphson algorithms using five iterations. The covariance matrix of the MLE is set and computed in the fourth step. The cost function of MLE method is constructed, and minimization problem is solved respectively on the fifth and sixth steps. Test of parameters convergence and validation are made respectively on seventh and eighth steps. Validation is made by plotting in common graph (I-V) or (P-V) curves from models and parameters extracted by MLE. At last, the obtained parameters are stored and will probably be used later for performance analysis, degradation analysis and diagnostics of PV generators.

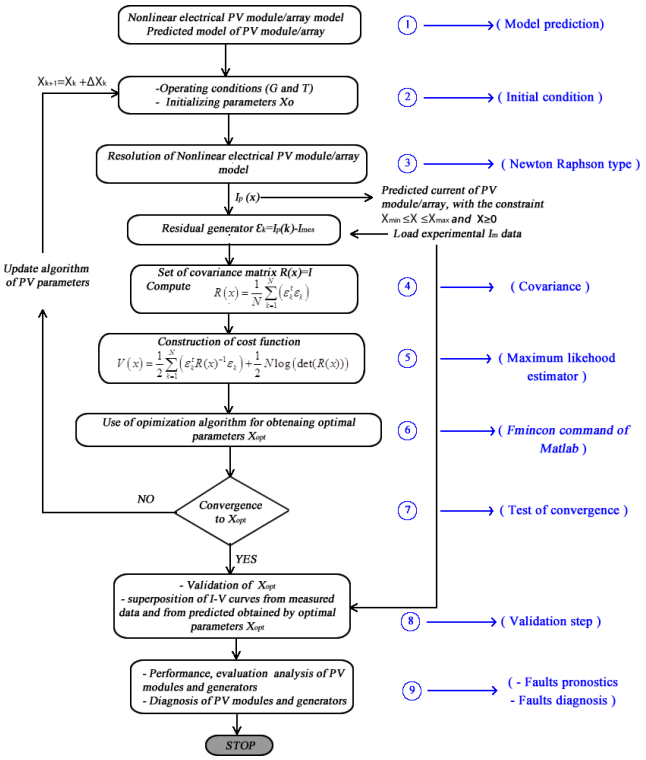

Figure 3. *Flowchart algorithm of parameters extraction using MLE.*

4.3. Details of Adopted Methodology Steps

A fault detection scheme for the PV modules is constructed by the proposed diagnosis and monitoring method. The method is based on the construction of the parameter residual generator Δx as mentioned by (15), and on the comparison between the measured (I-V) or (P-V) curves and the ones simulated from the estimated parameters.

Details on adopted methodology of faults diagnostic and monitoring, based on parameters estimation of single diode PV generator, using the MLE are shown in Figure 4. Parameters extraction is performed under standard test conditions (STC) or under nominal operating conditions test (NOCT).

Steps 8 and 9 of Figure 3 are important steps for detecting a fault. Based on these two steps, the diagnostic methodology (Figure 4) is built. The first step of the methodology is to evaluate and extract the parameters of a photovoltaic field without defects (no discolouration, no breaks on the panels, no defective cells...); this step is supposed to be at the beginning of its operations; these parameters are fixed as reference

parameters when the modules are without faults. The second step of the methodology consists of saving the extracted parameters at any time and compare them with the reference parameters measured at the beginning of the system operation. Here the comparison is carried out by calculating the residual vector and by plotting the curves resulting from the extracted parameters in common graphs. The comparative study of the residual vectors, and the curves make it possible to detect anomalies in the operation of the PV system. If $\Delta x = 0$ and the measured and estimated (P-V) curves are quite the same, then there are no anomalies in the PV generator. No faults are detected; the five parameters are stored to develop a long-term diagnostic analysis. If $\Delta x \neq 0$ and the measured and estimated (P-V) curves are different, a fault is detected. Then the estimated five parameters are not stored, and a short-term diagnostic procedure can be launched to identify the location and the type of the fault. Once the defects have been detected, the residual vector must be analyzed to know exactly the parameters which are not the same as the reference parameters; referring to section 2, this step makes it possible to locate the components that may be affected by these defects. Once the components (supposed faulty) located, it is necessary to evaluate the defects. This assessment allows us to know if the defects are majors or not; for major faults, it is important to go to a decision-making process to take corrective measures for avoiding a complete shutdown of the system. For minor faults, predictive or preventive maintenance must be carried out to anticipate more serious faults by using some protection methods.

This would enable the operator to act, to prevent the PV system under perform for prolonged periods of time, which improve the performance of the PV system by minimizing the power losses caused by the faults.

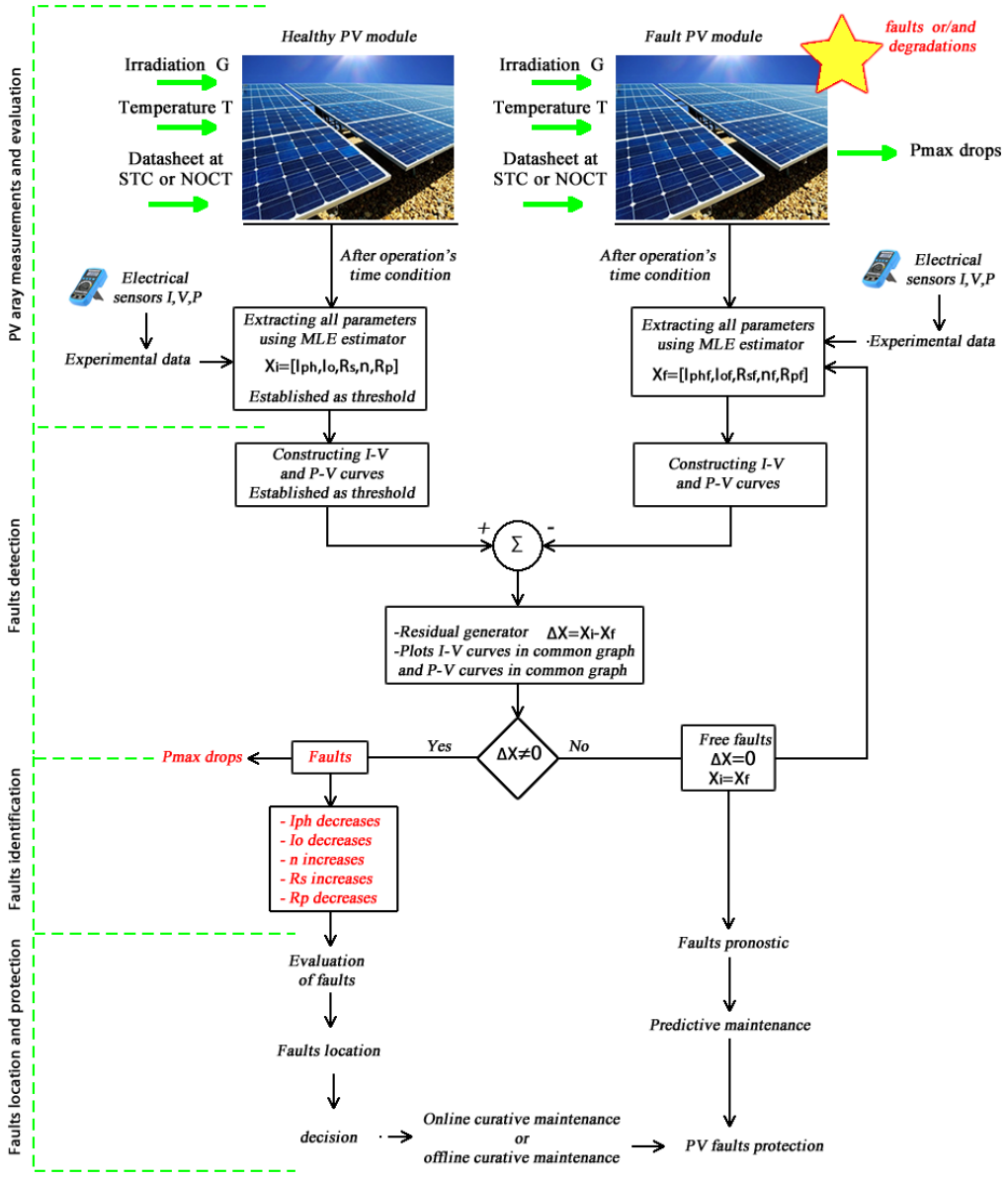

Figure 4. *Monitoring and Faults diagnosis methodology based on estimated parameters of single diode PV generators.*

5. Residual Generator, Faults Diagnosis and Monitoring Results and Discussion

In this section, simulation, and experimental results of the deviation detection of the parameters are presented, based on ARCO M75 modules. Table 3 shows the search range of the parameters NOCT by MLE. The calculated parameters are used not only to detect long-term defects (e.g., aging, soiling, delamination, etc.), but also to build the reference (I-V) curve when an impromptu fault happens (e.g., shading, breakdown diodes, etc.) and serious failures have occurred. Any deviation above the threshold or references (obtained in healthy cases) will significantly mean a degradation mode due to aging or failure caused by any mode of degradation or manufacturing defects if there is no protection. Any deviation of the parameters will immediately cause a variation of the (I-V) or (P-V) curve, hence modifying the maximum output power.

Table 2. *Search of five parameters of ARCO Solar M75 array at NOCT by MLE.*

Parameter	Rs (ohm)	Rp (ohm)	Iph (A)	Io (A)	n
Initial value	0.01	20	3	10^{-11}	1
Search range	0.005-0.7	20-600	2-4	10^{-13}-10^{-8}	1-2

Table 4. *Parameters of ARCO solar M75 array at NOCT in 1990, 2001, 2010.*

Parameters		Iph(A)	Io(A)	n	Rs(Ω)	Rp(Ω)	Isc (A)	Voc (V)	Pmax (W)
MLE	1990	3.299	10^{-8}	1.036	0.3	114.601	3.282	18.3	41.73
	2001	3.495	10^{-8}	1.020	0.328	25.630	3.449	18.01	39.43
	2010	2.987	10^{-8}	1.048	0.385	20.000	2.504	18	30.84
% /residual/ 1990-2001		5.94	0	1.54	44.5	77.63	5.08	1.58	5.51
% /residual/ 2001-2010		14.53	0	2.74	19.51	21.96	27.39	0.055	21.78
% /residual/ 1990-2010		9.45	0	1.15	34.96	82.54	23.70	1.63	26.09
Comments		Increase slightly and then decrease	constant	Decrease slightly and then increase	Increase slightly	decrease	Increase slightly and then decrease	decrease	decrease

As mentioned in monitoring and faults diagnosis methodology (Figure 4), firstly it is important to establish the references. So, the estimated curve and measured one (in the first year of operation 1990) is plotted in common graphs as illustrated in Figure 5. It is noticed the perfect matched between the two curves. So, at the PV modules in 1990 are considered as healthy PV modules and extracted parameters are set as references. Table 4 shows the extracted parameters for the three years of evaluation of the ARCO Solar M75 module by using MLE; It is observed that all residual vectors $\Delta x \neq 0$.

The first residual vector is established between the first year of operation and 2001 operation's year. It shows that the series resistance Rp (25.630 ohms) strongly decreases compared to the reference (114.601 ohms); the other parameters undergo slight modifications, all the same influencing the value of the short-circuit current (3.44 A), the open-circuit voltage (18.01 V) and the maximum power of the system (39.43 W). The maximum power thus suffers a loss of 5.51% compared to its reference value (41.73 W). The power and current curves from the extracted parameters and measured ones are plotted in common graph (Figure 6), slight discrepancies are observed at certain points between the estimated curves and those measured. When these curves are compared with those obtained in 1990, as illustrated in Figure 7, these curves are different at Isc, Voc, Pmax points. The decreased slope at Voc proves the existence of a high parasitic series resistance Rp. On the other hand, the small slope at Isc indicates high Rs and therefore a small parasitic shunt resistance. These offsets and differences between these curves are indicative of defects in the PV system.

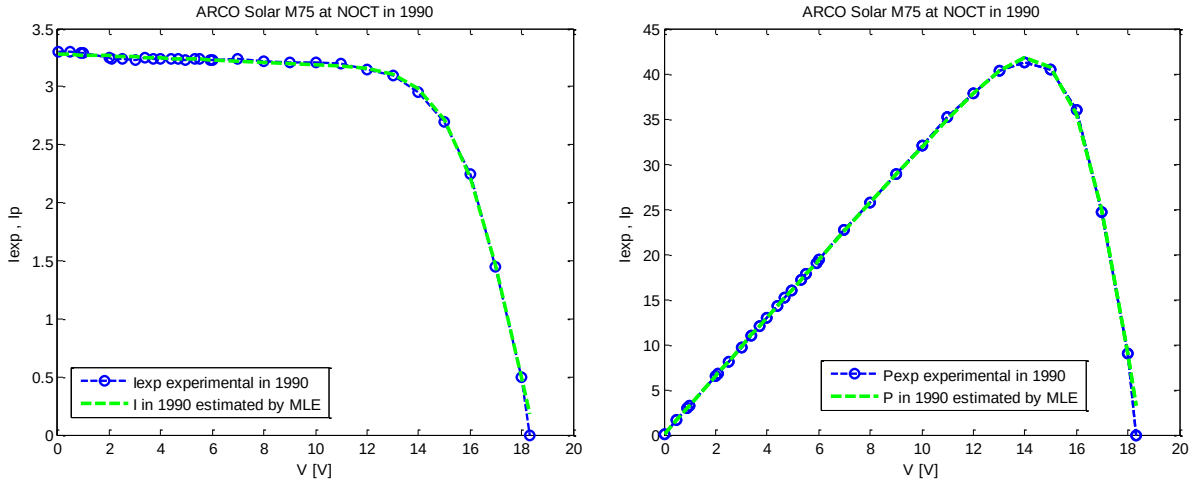

Figure 5. *ARCO Solar M75 curves in 1990.*

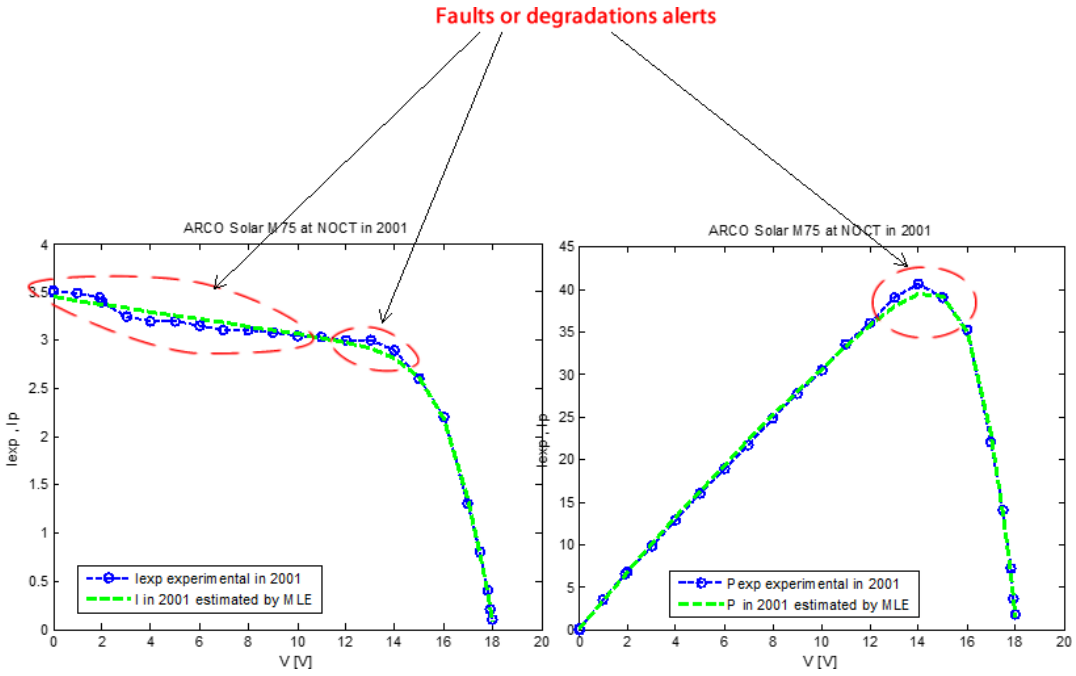

Figure 6. *ARCO Solar M75 curves in 2001.*

The second residual vector, evaluated between 2001 and 2010 years, shows that the series resistance Rp suffered a decrease of 21.96% compared to the value extracted in 2001. The shunt resistance undergoes an increase of 19.51% compared to the value extracted in 2001. The other parameters undergo slight variations Iph (14.53%), n (2.74%). Variations in the parameters influence the values of the short-circuit current (decreases by 27.39%), and the open-circuit voltage (decreases by 0.05%). The maximum power is thus 21.78% lower than its value in 2001 (39.43 W). The power and current curves from the extracted parameters and measured ones are plotted in common graph (Figure 8); they are completely different at most of all points. The decreased slope at Voc proves the existence of a high parasitic series resistance Rp. On the other hand, the small slope at Isc indicates high Rs and therefore a small parasitic shunt resistance. So, this observation indicates a significant defect in the PV system as illustrated in Figure 8. Thus, the I-V or P-V curve of the PV module shows that the deterioration in PV performance is mainly due to high resistance at the cell bus bars and contacts.

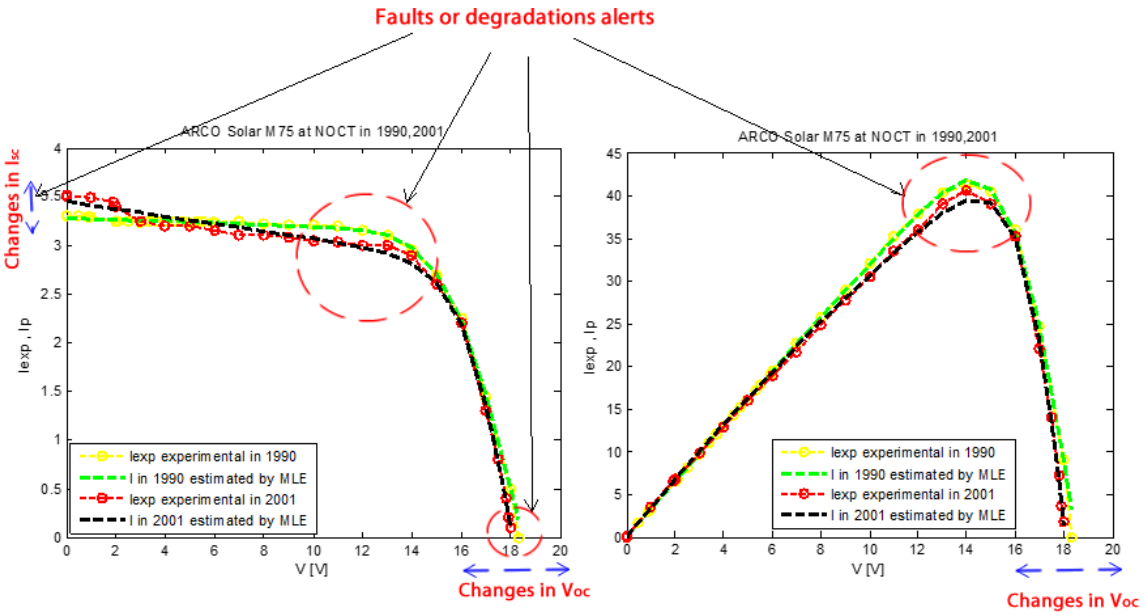

Figure 7. *ARCO Solar M75 curves in 1990, 2001 in common graph.*

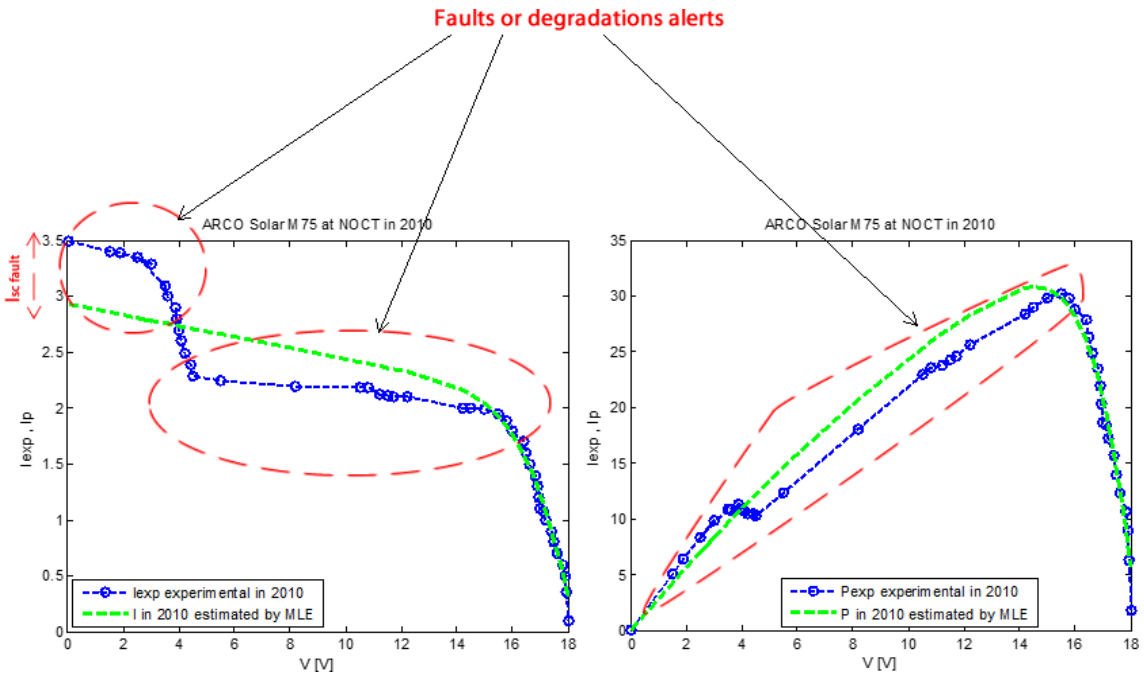

Figure 8. *ARCO Solar M75 curves in 2010.*

The 3rd residual vector, established between 1990 and 2010, is much more global from the beginning of operation until the last extraction carried out in 2010. Here it is found generally that all the parameters extracted undergo variations except saturation current Io. The parameters which vary more are the series resistance Rp (a modification of 82.54%), the shunt resistor Rs (a modification of 34.96%), the current of photon Iph (a modification of 9.45%); the ideality factor undergoes a slight change of 1.15%. The maximum power decreases by 26.09%.

An indication of the overall PV module performance degradation may be shown through the following observation: Rs increases slightly, Rp decreases, n increases, Io still constant. So, Voc decreases slightly, Isc decreases and Pmax drops. As mentioned in Section 3, parameters change typically result in power losses. It is observed that in 2010 the PV module lost about 26.09 % of its initial power. In the literature, the manufacturers consider that a PV module is degraded when its power reaches a level below 80% of its initial power [29]. Therefore, the PV modules under study is degraded. The fall of the maximum power is observed in Figure 9 where the curves are in the same graph for the three years. Analysis of

this figure shows that in 2001 and 2010 curves are not closed to the initial 1990 curves, which also leads to a detected malfunction of the ARCO M75 in those years.

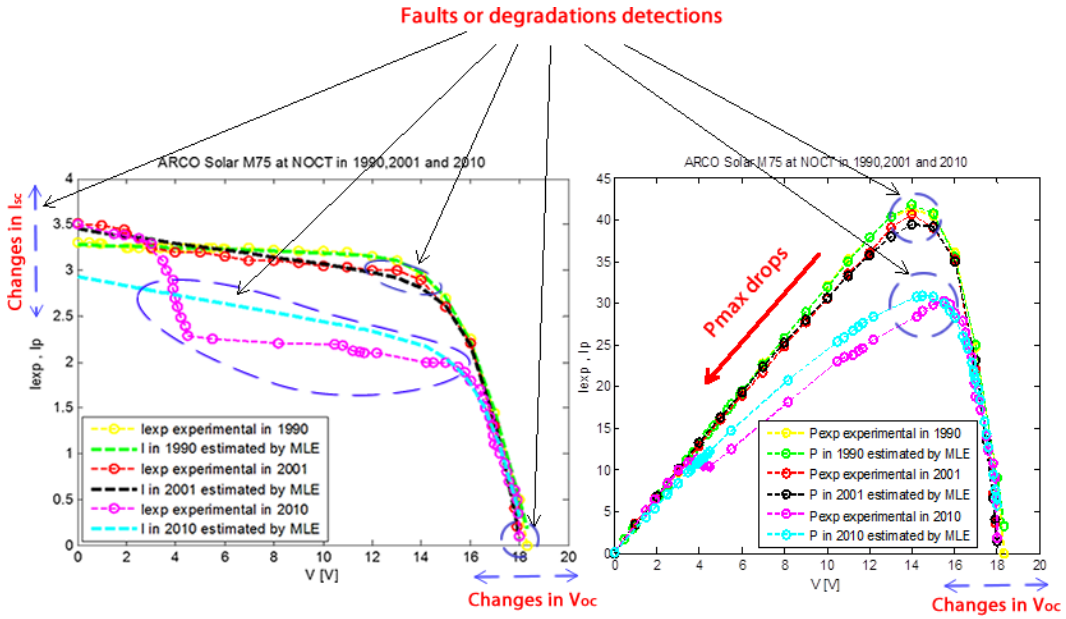

Figure 9. *ARCO Solar M75 curves analysis in 1990, 2001, 2010.*

The types of defects and faulty component related to parameter modifications were investigated in Section 4, which allows summarizing the different types of defects in this PV module from 1990 to 2010. Figure 10 summarizes the types of defects and faulty component of the PV system. So, it is recommended to act on the system through junction box, cell edges, wiring, busbars, and connectors.

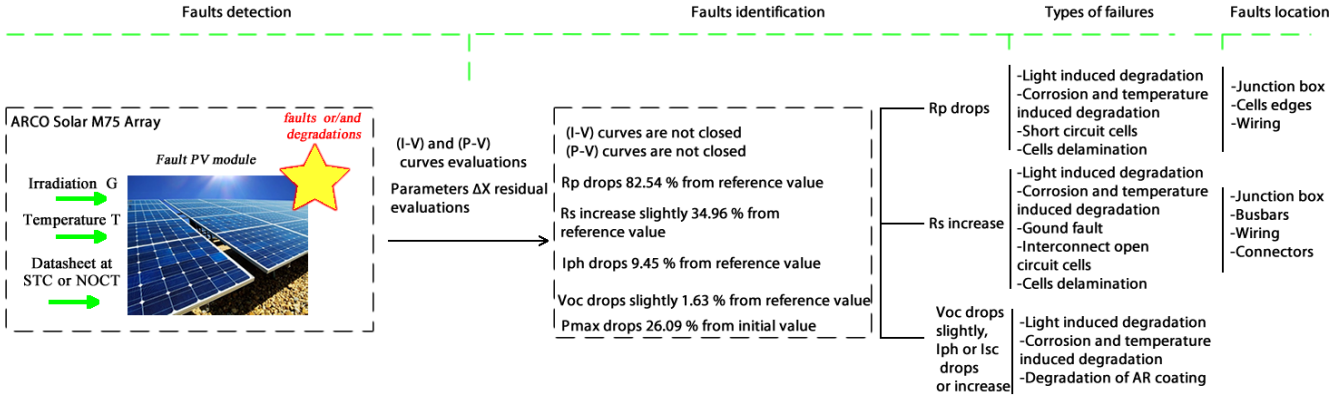

Figure 10. *Types of failures and faults location in ARCO Solar M75 on study.*

6. Conclusion

A method of fault detection and diagnostic of PV systems based on estimated parameters and (I-V) or (P-V) curves analysis in ARCO PV modules operating under field conditions already for 20 years has been presented in this paper. There is a perfect matched between the estimated and measured curves in 1990, so the PV modules in 1990 are considered as healthy PV modules and extracted parameters are set as references for analysis. Analysis of all residual vectors allows detection of defects in ARCO PV modules. From the first residual vector, the maximum power suffers a loss of 5.51% compared to its reference value (41.73 W), and slight discrepancies are observed at certain points between the estimated curves and those measured; from the second residual vector, the maximum power is 21.78% lower than its value in 2001 (39.43 W), and curves are different at most of all points; from 3rd residual vector, the maximum power decreases by

26.09%. It is observed that Rs increases slightly, Rp decreases, n increases, Io still constant. So, Voc decreases slightly, Isc decreases and Pmax drops. Finally, the types of defects and faulty components related to parameter modifications are listed in this work, and it is recommended to act to prevent severe faulty.

This approach brings several advantages in automatic defect diagnosis for remote inspection and monitoring of PV cell and module condition. The fault detection procedure can advantageously be integrated into a data acquisition system already installed in the PV plant. This sets up an intelligent monitoring and supervision system that can automatically give the operator an indication of faults. The addition of supervising systems for other system components, such as batteries and power conditioning units, complements a monitoring and control unit for the whole PV installation.

Abbreviations

PV	Photovoltaic
I	Current
V	Voltage
P	Power
I_{ph}	Photocurrent of PV Module/Array
$I_{ph,ref}$	Photocurrent of PV Module/Array at Reference Temperature
I_o	Saturation current of PV Module/Array
$I_{o,ref}$	Saturation current of PV Module/Array at Reference Temperature
$V_T = \frac{k_B T_\theta}{q}$	Thermal Voltage of a Photovoltaic Module/Array
$V_{T,ref}$	Thermal Voltage of a Photovoltaic Module/Array at Reference Temperature
n	The Diode Ideality Factor for a p-n Junction in a Cell
q	The Electron Charge ($1.602\times10^{-19} C$)
k_B	Boltzmann Constant ($1.38\times10^{-23} J/K$)
T_θ	The Absolute Temperature of the Module/Array
I_{mp}	Maximum Current
V_{mp}	Maximum Voltage
$P_{\max,e}$	Experimental Maximum Power
I_{sc}	Short Circuit Current
$I_{sc,ref}$	Short Circuit Current at Reference Temperature
V_{oc}	Open Circuit Voltage
$V_{oc,ref}$	Open Circuit Voltage at Reference Temperature
α_v	Temperature Coefficient of Voltage
α_I	Temperature Coefficient of Current
x_{opt}	Optimal Solution
STC	Standard Test Conditions
NOCT	Nominal Operating Condition Test
MLE	Maximum Likelihood Estimator
UV	Ultra Violet
FF	Fill Factor
EVA	Ethylene Vinyl Acetate

Author Contributions

Albert Ayang: Conceptualization, Formal Analysis, Methodology, Resources

Deli Goron: Formal Analysis, Methodology

Fabrice Kwefeu Mbakop: Formal Analysis, Methodology

Yaouba: Formal Analysis, Methodology, Writing – review & editing

Conflicts of Interest

The authors declare no conflicts of interests.

References

[1] S. Weckend, A. Wade, and G. Heath, "End-of-life management: Solar photovoltaic panels," National Renewable Energy Lab. (NREL), Golden, CO (United States), 2016.

[2] D. C. Jordan and S. R. Kurtz, "Photovoltaic degradation rates—an analytical review," *Progress in photovoltaics: Research and Applications*, vol. 21, no. 1, pp. 12-29, 2013.

[3] D. Jordan, *Methods of Analysis of Outdoor Performance Data*. National Renewable Energy Laboratory, 2011.

[4] P. Ducange, M. Fazzolari, B. Lazzerini, and F. Marcelloni, "An intelligent system for detecting faults in photovoltaic fields," in *2011 11th International Conference on Intelligent Systems Design and Applications*, 2011: IEEE, pp. 1341-1346.

[5] M. Davarifar, A. Rabhi, A. El-Hajjaji, and M. Dahmane, "Real-time model base fault diagnosis of PV panels using statistical signal processing," in *Renewable Energy Research and Applications (ICRERA), 2013 International Conference on*, 2013: IEEE, pp. 599-604. https://doi.org/10.1109/ICRERA.2013.6749826

[6] S. K. Firth, K. J. Lomas, and S. J. Rees, "A simple model of PV system performance and its use in fault detection," *Solar Energy*, vol. 84, no. 4, pp. 624-635, 2010. https://doi.org/10.1016/j.solener.2009.08.004

[7] A. Chouder and S. Silvestre, "Automatic supervision and fault detection of PV systems based on power losses analysis," *Energy conversion and Management*, vol. 51, no. 10, pp. 1929-1937, 2010. https://doi.org/10.1016/j.enconman.2010.02.025

[8] J. Solórzano and M. Egido, "Automatic fault diagnosis in PV systems with distributed MPPT," *Energy conversion and management*, vol. 76, pp. 925-934, 2013. http://dx.doi.org/10.1016/j.enconman.2013.08.055

[9] M. A. Ramli, S. Twaha, K. Ishaque, and Y. A. Al-Turki, "A review on maximum power point tracking for photovoltaic systems with and without shading conditions," *Renewable and Sustainable Energy Reviews*, vol. 67, pp. 144-159, 2017. https://doi.org/10.1016/j.rser.2016.09.013

[10] A. Ayang *et al.*, "Maximum likelihood parameters estimation of single-diode model of photovoltaic generator," *Renewable energy*, vol. 130, pp. 111-121, 2019. https://doi.org/10.1016/j.renene.2018.06.039

[11] A. Ayang, R. Wamkeue, M. Ouhrouche, and B. H. Malwe, "Maximum Likelihood Parameters Estimation Of Single-Diode Photovoltaic Module/Array: A Comparative Study At STC," in *2018 IEEE Electrical Power and Energy Conference (EPEC)*, 2018: IEEE, pp. 1-6. https://doi.org/10.1109/EPEC.2018.8598314

[12] J. Zoellick, "Testing and matching photovoltaic modules to maximize solar electric array performance "," *Senior project presented to the Department of Environmental Resources Engineering Humboldt State University*, 1990.

[13] A. M. Reis, N. T. Coleman, M. W. Marshall, P. A. Lehman, and C. E. Chamberlin, "Comparison of PV module performance before and after 11-years of field exposure," in *Photovoltaic Specialists Conference, 2002. Conference Record of the Twenty-Ninth IEEE*, 2002: IEEE, pp. 1432-1435.

[14] C. Chamberlin, M. Rocheleau, M. Marshall, A. Reis, N. Coleman, and P. Lehman, "Comparison of PV module performance before and after 11 and 20 years of field exposure," in *Photovoltaic Specialists Conference (PVSC), 2011 37th IEEE*, 2011: IEEE, pp. 000101-000105. https://doi.org/10.1109/PVSC.2011.6185854

[15] K. Park, G. Kang, H. Kim, G. Yu, and J. Kim, "Analysis of thermal and electrical performance of semi-transparent photovoltaic (PV) module," *Energy*, vol. 35, no. 6, pp. 2681-2687, 2010. https://doi.org/10.1016/j.energy.2009.07.019

[16] M. AlRashidi, M. AlHajri, K. El-Naggar, and A. Al-Othman, "A new estimation approach for determining the I–V characteristics of solar cells," *Solar Energy*, vol. 85, no. 7, pp. 1543-1550, 2011. https://doi.org/10.1016/j.solener.2011.04.013

[17] S. R. Wenham, *Applied photovoltaics*. Routledge, 2012. https://doi.org/10.4324/9781849776981

[18] S. Chattopadhyay *et al.*, "Visual degradation in field-aged crystalline silicon PV modules in India and correlation with electrical degradation," *IEEE Journal of photovoltaics*, vol. 4, no. 6, pp. 1470-1476, 2014.

[19] E. Kaplani, "Detection of degradation effects in field-aged c-Si solar cells through IR thermography and digital image processing," *International Journal of Photoenergy*, vol. 2012, 2012. https://doi.org/10.1155/2012/396792

[20] M. G. Villalva, J. R. Gazoli, and E. Ruppert Filho, "Modeling and circuit-based simulation of photovoltaic arrays," in *2009 Brazilian Power Electronics Conference*, 2009: IEEE, pp. 1244-1254.

[21] S. Alem-Boudjemline, "r éalisation et caract érisation de cellules photovolta ïques plastiques," 2004.

[22] M. Green, "Solar cells: operating principles, technology, and system applications. University of New South Wales, Kensington," *New South Wales, Australia*, pp. 96-97, 1992.

[23] S. Kadry, *Diagnostics and Prognostics of Engineering Systems: Methods and Techniques: Methods and Techniques*. IGI Global, 2012.

[24] F. Almonacid, C. Rus, P. P érez-Higueras, and L. Hontoria, "Calculation of the energy provided by a PV generator. Comparative study: conventional methods vs. artificial neural networks," *Energy*, vol. 36, no. 1, pp. 375-384, 2011. https://doi.org/10.1016/j.energy.2010.10.028

[25] M. Munoz, M. C. Alonso-Garc á, N. Vela, and F. Chenlo, "Early degradation of silicon PV modules and guaranty conditions," *Solar energy*, vol. 85, no. 9, pp. 2264-2274, 2011.

[26] V. Sharma and S. Chandel, "Performance and degradation analysis for long term reliability of solar photovoltaic systems: a review," *Renewable and Sustainable Energy Reviews*, vol. 27, pp. 753-767, 2013. https://doi.org/10.1016/j.rser.2013.07.046

[27] A. Charki, R. Laronde, and D. Bigaud, "The time-variant degradation of a photovoltaic system," *Journal of Solar Energy Engineering*, vol. 135, no. 2, p. 024503, 2013. https://doi.org/10.1115/1.4007771

[28] J. Wohlgemuth, D. W. Cunningham, A. Nguyen, G. Kelly, and D. Amin, "Failure modes of crystalline Si modules," in *PV Module Reliability Workshop*, 2010.

[29] A. Ndiaye, A. Charki, A. Kobi, C. M. K éb é, P. A. Ndiaye, and V. Sambou, "Degradations of silicon photovoltaic modules: A literature review," *Solar Energy*, vol. 96, pp. 140-151, 2013. http://dx.doi.org/10.1016/j.solener.2013.07.005

[30] J. H. Wohlgemuth and S. Kurtz, "Reliability testing beyond qualification as a key component in photovoltaic's progress toward grid parity," in *2011 International Reliability Physics Symposium*, 2011: IEEE, pp. 5E. 3.1-5E. 3.6.

[31] M. K. Al-Smadi and Y. Mahmoud, "Analysis of Photovoltaic Systems Power Losses in Partial Shading Conditions," in *IECON 2018-44th Annual Conference of the IEEE Industrial Electronics Society*, 2018: IEEE, pp. 1699-1704. https://doi.org/10.1109/IECON.2018.8591806

[32] D. S. Pillai and N. Rajasekar, "A comprehensive review on protection challenges and fault diagnosis in PV systems," *Renewable and Sustainable Energy Reviews*, vol. 91, pp. 18-40, 2018. https://doi.org/10.1016/j.rser.2018.03.082

[33] S. R. Madeti and S. Singh, "A comprehensive study on different types of faults and detection techniques for solar photovoltaic system," *Solar Energy*, vol. 158, pp. 161-185, 2017. https://doi.org/10.1016/j.solener.2017.08.069

[34] A. Triki-Lahiani, A. B.-B. Abdelghani, and I. Slama-Belkhodja, "Fault detection and monitoring systems for photovoltaic installations: A review," *Renewable and Sustainable Energy Reviews*, vol. 82, pp. 2680-2692, 2018. https://doi.org/10.1016/j.rser.2017.09.101

[35] A. Mellit, G. M. Tina, and S. A. Kalogirou, "Fault detection and diagnosis methods for photovoltaic systems: A review," *Renewable and Sustainable Energy Reviews*, vol. 91, pp. 1-17, 2018. https://doi.org/10.1016/j.rser.2018.03.062